Synthesis of micro-sized titanium dioxide nanosheets wholly exposed with high-energy {001} and {100} facets

Author

Wen, Ci Zhang, Zhou, Ji Zhi, Jiang, Hai Bo, Hu, Qiu Hong, Qiao, Shi Zhang, Yang, Hua Gui

Published

2011

Journal Title

Chemical Communications

DOI

10.1039/C0CC05798C

Synthesis of Micro-Sized Titanium Dioxide Nanosheets Wholly Exposed with High-Energy {001} and {100} Facets

Ci Zhang Wen[a], Ji Zhi Zhou[b], Hai Bo Jiang[a], Qiu Hong Hu[b], Shi Zhang Qiao*[b], Hua Gui Yang*[a]

Received (in XXX, XXX) Xth XXXXXXXXX 200X, Accepted Xth XXXXXXXXX 200X
First published on the web Xth XXXXXXXXX 200X
DOI: 10.1039/b000000x

A new synthetic strategy was developed to prepare large-sized well-defined anatase TiO_2 nanosheets wholly dominated with thermodynamically unfavorable high-reactive {001} and {100} facets, which has a percentage of 98.7% and 1.3%, respectively. The as-prepared anatase TiO_2 nanosheets show a well-faceted morphology and have a large size in length (*ca.* 4.14 μm). The formation mechanism of the anatase TiO_2 nanosheets was also analyzed and investigated.

In recent years, intensive research attention has been paid to design and synthesis of functional inorganic crystals with exposed high-energy surfaces, which normally show excellent physiochemical properties because of their unique geometrical and electronic structures such as high densities of atom steps, kinks, dangling bonds, and ledges.[1-3] Titanium dioxide (TiO_2) has been extensively studied due to its many industrial applications such as photovoltaic cells, photo-/electrochromics, photocatalysis, photonic crystals, smart surface coatings, rechargeable lithium batteries, sensors, and so on.[4-8] For anatase TiO_2, both theoretical and experimental studies found that both {001} and {100} facets in the equilibrium state are especially reactive.[9] Unfortunately, due to the minimization of surface energy during the process of crystal growth, most available anatase TiO_2 nanocrystals were dominated by the thermodynamically stable {101} facets other than the more reactive {001} or {100} facets (0.90 J/m^2 for {001}; > 0.53 J/m^2 for {100}; > 0.44 J/m^2 for {101}).[9-11]

On the basis of theoretical predictions, for the first time we have successfully synthesized uniform anatase TiO_2 single crystals with a high percentage (47 – 64%) of {001} facets using hydrofluoric acid as a morphology controlling agent.[12,13] Following these breakthroughs, various reaction systems or capping agents have been recently exploited to achieve TiO_2 with exposed high-reactive {001} and {100} facets.[14-21] For instance, by hydrothermal reaction of tetrabutyl titanate and hydrofluoric acid (HF), Han et al.[14] synthesized nano-sized sheet-like anatase TiO_2 with up to 89% of {001} facets and average size length of 30 – 130 nm, which showed superior photocatalytic performance. Furthermore, by using Na-titanate nanotubes as solid precursor, TiO_2 single crystals with active {100} facets have recently prepared under hydrothermal conditions.[16]

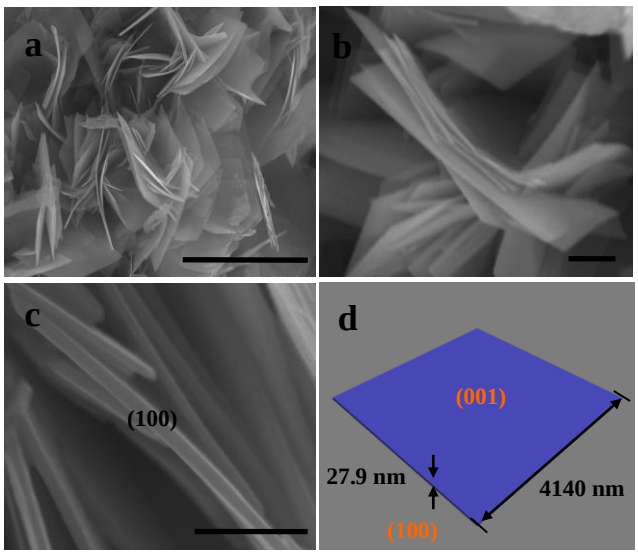

Fig. 1 a), b) and c) FESEM images of anatase TiO_2 nanosheets synthesized at 210 °C for 24 h. d) Schematic structure of the as-obtained anatase TiO_2 nanosheets. Scale bars in (a-c) are 5.0 μm, 2.0 μm, and 300 nm, respectively.

Just like one-atom-thick planar graphene sheet, active-surface dominated anatase TiO_2 nanosheets might extend many applications of this important semiconducting material. Even though anatase TiO_2 with dominant {001} or {100} was prepared recently, to the best of our knowledge, preparing well-faceted anatase TiO_2 single crystalline nanosheets wholly exposed with {001} and {100} facets have not been synthesized so far. Both theoretical predictions and experimental results indicates that hydroxyl groups can lower the surface energy of {100} facets significantly and the oxygenated surface may lead to formation of {100} facets, which means that only in basic conditions can {100} facets be formed. On the other hand, previous experimental results testified that {001} facets were generally generated under acidic conditions. Thus preparing anatase TiO_2 exposed by {001} and {100} facets instead of thermodynamically stable

[a] *Key Laboratory for Ultrafine Materials of Ministry of Education, School of Materials Science and Engineering, East China University of Science and Technology, 130 Meilong Road, Shanghai 200237 China; Fax: 86 21 64252127; Tel: 86 21 64252127; E-mail: hgyang@ecust.edu.cn*
[b] *The University of Queensland, ARC Centre of Excellence for Functional Nanomaterials, Australian Institute for Bioengineering and Nanotechnology, QLD 4072, Australia; Fax: 61 7 33463973; Tel: 61 7 33463815; E-mail: s.qiao@uq.edu.au*

† Electronic Supplementary Information (ESI) available: Experimental details, XRD, Raman spectra, XPS, SEM images of the as-obtained $TiOF_2$ and photocatalytic property for H_2 generation.

low-reactive {101} facets is highly desired and still remains a challenge. Furthermore, because of the low structural stability of high-active surface during the crystal growth process (i.e., 1 x 4 reconstruction), for ultrathin anatase TiO_2 nanosheets dominated with {001} facets, the length along [100] crystallographic direction is only around 100 nm and it is thus also quite challenging to prepare well-faceted large-sized anatase TiO_2 nanosheets, which might have great potential applications.

Herein we report a facial synthetic method for the preparation of large-sized anatase TiO_2 nanosheets wholly dominated with high-reactive {001} and {100} facets, which have percentages of 98.7% and 1.3%, respectively. The as-prepared anatase TiO_2 nanosheets show a well-faceted morphology and have a unique large size in length (*ca*. 4.14 μm). The formation mechanism of the anatase TiO_2 nanosheets entirely dominated by high-reactive crystallographic facets is also discussed using the experimental results of early reaction stage.

Large-sized anatase TiO_2 nanosheets wholly exposed with high-energy {001} and {100} facets were prepared through a solvothermal route at 210 ºC for 18-24 h, wherein titanium tetrafluoride (TiF_4) was transferred to titanium oxydifluoride ($TiOF_2$) first and then anatase TiO_2 in 20 mL of 1-butanol ($CH_3(CH_2)_2CH_2OH$) solvent containing 0.2 mL of 48% HF. The crystallographic structure of the resulting products was evidenced by powder X-ray diffraction (XRD) (will be discussed in Fig. S1a), which reveals a phase-pure anatase TiO_2 (space group $I4_1/amd$, JCPDS No. 21-1272).[21] Fig. 1 shows the typical results of our field-emission scanning electron microscopy (FESEM) investigations. Low-magnification SEM images in Fig. 1a and b show the general morphology of the paper-like anatase TiO_2 nanosheets which have a micro-size and also demonstrate some flexibility. In a high-magnification SEM image, the edges of these anatase TiO_2 nanosheets are quite flat and smooth (see Fig. 1c), indicating that the edges should only contain one type of crystallographic facet. More SEM evidence is provided in Fig. S2, which indicates the same results. On the basis of the symmetries of anatase TiO_2, the square surfaces must be {001} facets and the other four rectangle surfaces are {100} facets of the anatase TiO_2 single crystals (further evidence is given in Fig. 2). The yield of anatase TiO_2 nanosheets is nearly 100%, even though some agglomerates were occasionally observed. To examine the uniformity of the synthesized anatase TiO_2 nanosheets, the values of length and thickness of anatase TiO_2 nanosheets were statistically analyzed. The average value of length is 4.14 μm and the thickness is only 27.9 nm. Thus we estimate the percentages of {001} and {100} facets to be 98.7% and 1.3%, respectively. A schematic morphology of the as-synthesized anatase TiO_2 nanosheets is also provided in Fig. 1d and the values of the length and thickness are all proportional to the experimental results.

The results of transmission electron microscopy and selected-area electron diffraction (TEM/SAED) of anatase TiO_2 nanosheets dominated with high-energy {001} and {100} facets are shown in Figs. 2 a-d. The selected-area electron diffraction patterns can be indexed into diffraction spots of

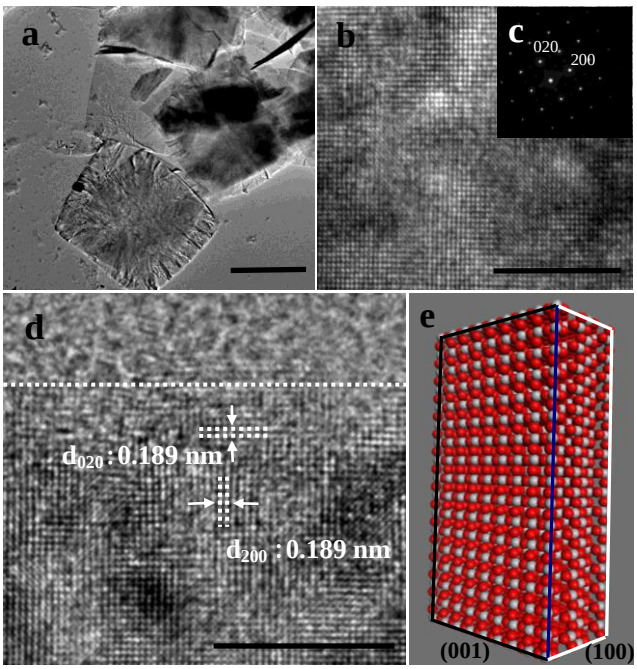

Fig. 2 a) TEM image of the anatase TiO_2 nanosheets obtained at 210 ºC for 20 h. b) and c) HRTEM image and SAED pattern of the anatase TiO_2 nanosheets (recorded on the central region of a free standing nanosheet). d) HRTEM image of anatase TiO_2 nanosheets, which was recorded on the edge region. e) Schematic atomic model of the {100} and {001} boundary of anatase TiO_2 nanosheets. Scale bars in a), b) and d) are 3.0 μm, 5.0 nm, and 5.0 nm, respectively.

the [001] zone.[21] The high-resolution TEM image (Fig. 2b) in the central area of a free-standing anatase TiO_2 nanosheet shows the (200) and (020) atomic planes with a lattice spacing of 1.89 Å and an interfacial angle of 90º. More importantly, the high-resolution TEM image of the edge region (Fig. 2d) also indicates a relatively high crystallinity and well-faceted surface; this implies that the boundary between (001) and (100) surface is well constructed, which can be mimicked by the schematic structure shown in Fig. 2e. Moreover, Raman spectroscopy was applied to examine the crystal phase of anatase TiO_2 nanosheets and the results show typical Raman spectrum of anatase TiO_2 which has six modes appearing at 144 cm^{-1} (E_g), 197 cm^{-1} (E_g), 399 cm^{-1} (B_{1g}), 513 cm^{-1} (A_{1g}), 519 cm^{-1} (B_{1g}), and 639 cm^{-1} (E_g) (see Supporting Information, Fig. S3).[22] This finding is also consistent with XRD results shown in Fig. S1a. In order to study the formation mechanism of the large-sized anatase TiO_2 nanosheets wholly dominated with high-reactive {001} and {100} facets, the products at early reaction stage were collected and analyzed systematically. As indicated in Figs. 1, 2 and S1a, the TiO_2 products with a reaction time of 18 – 24 h are only in pure anatase polymorph. However, under the same reaction media, if the reaction time is shorter than 17 h, only $TiOF_2$ crystals can be found (see Supporting Information, Fig. S4). XRD pattern in Fig. S1b clearly illustrates the pure cubical $TiOF_2$ phase (space group $Pm3m$, JCPDS No. 08-

0060).

The morphology of early stage products (cubical $TiOF_2$ crystals) with a reaction time of 6 h was studied using SEM (Supporting Information, Fig. S4). From the symmetries of cubic $TiOF_2$ crystals, all the flat, square surfaces can be indexed into {100} facets. These well-faceted crystals show an average length of 4.3 μm, which is quite comparable to that of the final anatase TiO_2 nanosheets. From these results, it can be proposed that $TiOF_2$ is an important intermediate product and may play an important role in the formation of our unique anatase TiO_2 nanosheets. All the results indicate that the $TiOF_2$ is the only product on the first reaction stage and then it dissolve gradually into the solvent. Only after this stage, can anatase TiO_2 nanosheets begin to appear in the solid precipitates (Supporting Information, Fig. S5).

More importantly, Barnard *et al* have theoretically proved that for anatase TiO_2, hydroxyl can lower the surface energy of {100} facets and the oxygenated surface may lead to appearance of {100} facets with a significant percentage.[3] However, our synthetic condition is very different from these theoretical assumptions, which generally is in basic reaction medium. Thus the formation of high-energy {100} facets in this work might be attributed to a different strategy. The lattice constants between the (100) plane of cubic $TiOF_2$ (space group *Pm3m*, a,b,c = 3.798 Å) and the (100) plane of tetragonal anatase TiO_2 (space group *I*41/*amd*, a,b = 3.7852 Å and c = 9.5139 Å) is quite close along the [001] direction and the lattice mismatch is only 0.34% for {100} facets of $TiOF_2$ and anatase TiO_2. This structural resemblance may be the root cause of the formation of {100} facets in the large-sized anatase TiO_2 nanosheets (overall percentage = 1.3%) other than thermodynamically stable {101} facets. That is, the solid $TiOF_2$ acts as rigid "hard templates" to generate the thermodynamically unfavorable crystal facets of anatase TiO_2. The hydrogen (H_2) evolution rate from photochemical reduction of water by using the products with a reaction time of 24 h (see Fig. S6 and S7 in Supporting Information) was also tested and the enhanced property might be attributed to the existence of high-reactive {001} and {100} facets.

In summary, large anatase TiO_2 nanosheets wholly dominated by high-reactive {001} and {100} facets were synthesized by a solvothermal route. The adsorption of HF on the crystal surface determines the high percentage of {001} facets while the perfect lattice match between anatase TiO_2 and $TiOF_2$ along [100] crystallographic direction promote the generation of high-energy of {100} facets instead of other thermodynamically facets such as {101} of anatase TiO_2. The as-synthesized products exhibit superior photocatalytic property in contrast with the sample with 47% {001} facets. Besides the traditional applications in the areas such as environment and clean energy, the unique lamellar structure of anatase TiO_2 prepared in this work might pave the way to extend the applications of TiO_2 into other areas such as functional coatings, devices, or model samples for fundamental surface science. Furthermore, the present work also motivates us to explore new synthetic methods for the preparation of tailored crystal facets of other functional metal oxides.

Notes and references

This work was financially supported by Pujiang Talents Programme and Major Basic Research Programme of Science and Technology Commission of Shanghai Municipality (09PJ1402800, 10JC1403200), Shuguang Talents Programme of Education Commission of Shanghai Municipality (09SG27), National Natural Science Foundation of China (20973059, 91022023, 21076076, 21073060), Fundamental Research Funds for the Central Universities (WJ0913001) and Program for New Century Excellent Talents in University (NCET-09-0347) and the Australian Research Council (ARC) through Discovery Project program (DP1095861, DP0987969).

1. N. Tian, Z. Y. Zhou, S. G. Sun, Y. Ding, Z. L. Wang, *Science*, 2007, **316**, 732.
2. X. G. Han, M. S. Jin, S. F. Xie, Q. Kuang, Z. Y. Jiang, Y. Q. Jiang, Z. X. Xie, L. S. Zheng, *Angew. Chem. Int. Ed.*, 2009, **48**, 9180.
3. A. S. Barnard, L. A. Curtiss, *Nano Lett.*, 2005, **5**, 1261.
4. A. Fujishima, K. Honda, *Nature*, 1972, **238**, 37.
5. M. Grätzel, *Nature*, 2001, **414**, 338.
6. A. L. Linsebigler, G. Lu, J. T. Yates, *Jr. Chem. Rev.*, 1995, **95**, 735.
7. J. S. Chen, X. W. Lou, *Electrochemistry Communications*, 2009, **11**, 2332.
8. S. W. Liu, J. G. Yu, M. Jaroniec, *J. Am. Chem. Soc.*, 2010, **132**, 11914.
9. X. Q. Gong, A. Selloni, *J. Phys. Chem. B*, 2005, **109**, 19560.
10. M. Lazzeri, A. Vittadini, A. Selloni, *Phys. Rev. B*, 2001, **63**, 155409.
11. M. Lazzeri, A. Vittadini, A. Selloni, *Phys. Rev. B*, 2002, **65**, 119901.
12. H. G. Yang, C. H. Sun, S. Z. Qiao, J. Zou, G. Liu, S. C. Smith, H. M. Cheng, G. Q. Lu, *Nature*, 2008, **453**, 638.
13. H. G. Yang, G. Liu, S. Z. Qiao, C. H. Sun, Y. G. Jin, S. C. Smith, J. Zou, H. M. Cheng, G. Q. Lu, *J. Am. Chem. Soc.*, 2009, **131**, 4978.
14. X. G. Han, Q. Kuang, M. S. Jin, Z. X. Xie, L. S. Zheng, *J. Am. Chem. Soc.*, 2009, **131**, 3152; J. G. Yu, L. F. Qi and M. Jaroniec, *J. Phys. Chem. C*, 2010, **114**, 13118; Q. J. Xiang, K. L. Lv and J. G. Yu, *Appl. Catal. B: Environ*., 2010, **96**, 557; Z. K. Zheng, B. B. Huang, X. Y. Qin, X. Y. Zhang, Y. Dai, M. H. Jiang, P. Wang and M. H. Whangbo, *Chem. Eur. J.*, 2009, **15**, 12576; G. Mogilevsky, Q. Chen, H. Kulkarni, A. Kleinhammes, W. M. Mullins and Y. Wu, *J. Phys. Chem. C*, 2008, **112**, 3239; J. G. Yu, J. J. Fan and K. L. Lv, *Nanoscale*, 2010, **2**, 2144; J. S. Chen, Y. L. Tan, C. M. Li, Y. L. Cheah, D. Luan, S. Madhavi, F. Y. C. Boey, L. A. Archer and X. W. Lou, *J. Am. Chem. Soc.*, 2010, **132**, 6124; X. G. Han, Q. Kuang, M. S. Jin, Z. X. Xie and L. S. Zheng, *J. Am. Chem. Soc.*, 2009, **131**, 3152.
15. J. S. Chen, Y. L. Tan, C. M. Li, Y. L. Cheah, D. Y. Luan, S. Madhavi, F. Y. C. Boey, *J. Am. Chem. Soc.*, 2010, **132**, 6124.
16. J. M. Li, D. S. Xu, *Chem. Commun*., 2010, **46**, 2301.
17. D. Q. Zhang, G. S. Li, X. F. Yang, J. C. Yu, *Chem. Commun.*, 2009, 4381.
18. M. Min, L. Y. Piao, L. Zhao, S. T. Ju, Z. J. Yan, T. He, C. L. Zhou, W. J. Wang, *Chem. Commun.*, 2010, **46**, 1664.
19. G. Liu, H. G. Yang, X. W. Wang, L. N. Chen, H. F. Lu, L. Z. Wang, G. Q. Lu, H. M. Cheng, *J. Phys. Chem. C*, 2009, **113**, 21784.
20. F. Amano, O. O. Prieto-Mahaney, Y. Terada, T. Yasumoto, T. Shibayama, B. Ohtani, *Chem. Mater*., 2009, **21**, 2601.
21. H. G. Yang, H. C. Zeng, *J. Phys. Chem. B*, 2004, **108**, 3492.
22. T. Ohsaka, *J. Phys. Soc. Jpn.*, 1980, **48**, 1661.